Commun. Comput. Phys.
doi: 10.4208/cicp.220612.071112a

Vol. **14**, No. 3, pp. 703-721
September 2013

Employing Per-Component Time Step in DSMC Simulations of Disparate Mass and Cross-Section Gas Mixtures

Roman V. Maltsev*

8-22, Koltsovo, Novosibirsk, 630559, Russia.

Received 22 June 2012; Accepted (in revised version) 7 November 2012

Communicated by Sauro Succi

Available online 6 February 2013

Abstract. A new approach to simulation of stationary flows by Direct Simulation Monte Carlo method is proposed. The idea is to specify an individual time step for each component of a gas mixture. The approach consists of modifications mainly to collision phase simulation and recommendations on choosing time step ratios. It allows lowering the demands on the computational resources for cases of disparate collision diameters of molecules and/or disparate molecular masses. These are cases important e.g., in vacuum deposition technologies. Few tests of the new approach are made. Finally, the usage of new approach is demonstrated on a problem of silver nanocluster diffusion in argon carrier gas under conditions of silver deposition experiments.

AMS subject classifications: 65C05, 76M28

Key words: Direct Simulation Monte Carlo, time step, disparate masses, gas mixture, nanoclusters.

1 Introduction

The Direct Simulation Monte Carlo (DSMC) method [1] is a standard for the simulation of nonequilibrium rarefied gas flows described by the Boltzmann equation. This method is based on tracking individual molecules (simulators), considering them moving independently with occasional discrete events of pair collisions applied according to a statistical model. After the steady state is reached, the average of simulator parameters over many time steps delivers macroparameters of the flow. The method has three discretization parameters:

*Corresponding author. *Email address:* rmaltsev@gmail.com (R. V. Maltsev)

First, displacement and collision phase are uncoupled to speed up a computation, this defines the time step parameter Δt.

Second, a considerably limited, reduced number of simulators is used to simulate a large number of physical molecules. The symmetry of the Boltzmann equation allows reducing the number density n of molecules by increasing the collision cross-section σ_T, keeping the local mean free path λ unchanged:

$$n \to \frac{n}{F}, \qquad \sigma_T \to F\sigma_T, \qquad \lambda = \frac{1}{\sqrt{2}n\sigma_T},$$

here F is the number of physical molecules represented by a simulator.

Third, for a reduced number of simulators, collisions can no longer be a point event, as it should in the Boltzmann equation, so, the simulation area is divided into cells of linear size h and collision partners are chosen randomly within the same cell, causing spatial collision separation.

As is said, DSMC is the most practical method for the numerical simulation of nonequilibrium rarefied gas flows. However, the statistical nature of DSMC forces to calculate a lot of time steps to collect enough samples to get good statistical averages, as the noise amplitude is inversely proportional to the square root of the simulated period of time. When the flow is close to equilibrium, gradients of macroparameters are too small to resolve. This forces to use modified DSMC [2–5] or even alternative [6, 7] methods to solve the Boltzmann equation.

Discretization causes distortion of flow parameters and effective transport coefficients, the error is of second order in cell size and time step, i.e., $\sim (h/\lambda)^2$ [8] and $\sim (v_C\Delta t)^2$ [9] (v_C is the local mean collision frequency) and first order in F, i.e., $\sim h/(\lambda\overline{N})$ [10] ($\overline{N}$ is the mean number of simulators in a cell and $\lambda\overline{N}$ is invariant on local density). Simulating a d-dimensional flow of characteristic linear size L and characteristic mean free path λ, keeping the same distortion, requires $\sim(L/\lambda)^d$ cells and a proportional number of simulators, these determine demands on computer memory and on number of operations per time step. With the increase of flow density, the time step has to shrink, while relaxation of the flow slows down, therefore, the number of time steps to reach steady state is $\sim(L/\lambda)^2$. Sometimes reaching a steady state is more costly than collecting a good average of flow properties. When reaching a steady state is not obvious, convergence detection algorithms have to be used [11].

The majorant collision frequency (MCF) scheme [12] assumes that each possible pair (i,j) of simulators in a cell has its own collision frequency:

$$v_{ij} = \frac{F\sigma_T c_r}{V_C}, \tag{1.1}$$

here c_r is the relative velocity and V_C is the cell volume. The algorithm to accomplish this is as following. First, a value of the majorant collision frequency $v_{\max}$ is chosen in each

cell:

$$v_{\max} = \frac{F\{\sigma_T c_r\}_{\max}}{V_C}.$$

The value $v_{\max}$ is to be high enough, so that only a negligible fraction of pairs exceeds it. In practice, the local value of $v_{\max}$ is updated each time it is exceeded. The majorant frequency is used to calculate the expected number of virtual collisions:

$$\overline{K_{\max}} = \frac{N(N-1)}{2} v_{\max} \Delta t,$$

here N is a present number of simulators in a cell. The actual number $K_{\max}$ of virtual collisions is a sample from a Poisson distribution with mean value $\overline{K_{\max}}$. Then, $K_{\max}$ random collision pairs are chosen within a cell, each virtual collision is accepted (and simulated) with probability $v_{ij}/v_{\max}$.

In contrast to the original No Time Counter (NTC) scheme [1], a priori knowledge of the mean number $\overline{N}$ of simulators in a cell is not required and does not need to be evaluated on-the-fly. This makes the MCF scheme insensitive to $\overline{N}$ [10], in contrast to the original NTC scheme [13]. In a later version of the NTC scheme, Bird proposed to use the same $\overline{K_{\max}}$ as in the MCF scheme, but with $K_{\max}$ calculated as $\overline{K_{\max}}$ randomized to one of two nearest integers, rather than sampling from a Poisson distribution.

The usage of the MCF scheme is supposed everywhere in this paper.

Component weights. Sometimes in simulations, the concentration of some component is too small to collect good averages. A solution is to use a smaller value of F (simulator weight) for a scanty component only, to increase a number of simulators reasonably. Using a small F for all components would increase the number of simulators enormously. However, the collision scheme must be modified [14] for colliding simulators of different weights. Eq. (1.1) then becomes:

$$v_{ij} = \frac{\max\{F_i, F_j\}\sigma_T c_r}{V_C}, \tag{1.2}$$

here F_i is the component weight of simulator i. If the collision is accepted, simulator i changes its parameters to post-collision ones with the probability $F_i/\max\{F_i, F_j\}$. Hence, a simulator with smaller weight always receives post-collision parameters, another one may either receive post-collision or retain pre-collision parameters. This non-symmetry brings a number of drawbacks. First, the scheme is non-conservative, so, random walks of momentum and energy are present. Second, the simulator with smaller weight may collide with the same pre-collision simulator of greater weight again. This causes a specific distortion of the distribution function[†]. This distortion decreases as more simulators (especially for components of greater weight) are used, or as component weights become

[†]Explicit rejection of such collisions helps, but does not solve the problem of specific distortion completely.

less distinct. If the component of smaller weight also has much greater mass, it is severely sensitive to this distortion.

Spatial weights. A simulator weight F can depend on coordinates. However, simulators have to be duplicated/decimated when they travel between regions with different F. Spatial weights retain all drawbacks of component weights. Additionally, randomization in duplication/decimation scheme causes random walks of density, sometimes severe [15]. Nevertheless, the particular case of radial weights is almost indispensable for axisymmetric flows. Otherwise, there are too few simulators near the axis and too many on the periphery.

Kannenberg's approach. In some flows, the density can vary by orders of magnitude. Lower density regions may be correctly simulated with larger cells, longer time step and larger F, i.e., fewer simulators[‡]. Kannenberg proposed an approach [16] to take advantage of this, though it works only for stationary flows. Let us introduce the time step scaling factor T in each simulation cell, with local time step becoming $T\Delta t$, while now Δt is the reference global time step. The local time step is used in both transposition and collision phases. In transposition phase, when a simulator moves to a cell with different corresponding T, it retains the unused fraction of the time step, i.e., the absolute residue of time step adjusts to the new value of T. Additionally, local values of F are scaled in proportion to T, so, the ratio $W=F/T$ retains the same in all cells (W will be called the combined weight later on). Duplication/decimation is not needed in the case $W=const$, as simulators tend to crowd more in cells of smaller time step, naturally. The collision frequency of a pair (1.1) with respect to the global time step now may be written in the form:

$$v_{ij}=T^2\frac{W\sigma_T c_r}{V_C}, \tag{1.3}$$

where the first incarnation of T converts W to F, and the second one scales the global time step.

To apply the approach, first, larger cells are to be chosen in the region of lower density. Then, local F and T are increased. Amount of increase is limited by allowing neither $h/(\lambda\overline{N})$, nor $v_C T\Delta t$ discretization indexes exceed their preferred values.

Adapting the local time step gives a triple advantage. First, it decreases the total number of simulators required. Second, it locally accelerates the convergence toward the steady state in low-density regions. Third, a decreasing number of simulators does not harm the statistical convergence, as intra-cell correlations now decay faster, balancing the reduction in number of simulators. All these facts decrease demands on computational resources without detriment to precision.

Despite symmetrical collisions, the approach is not strictly conservative, as the mass, momentum and energy may redistribute among simulators of different F. This causes inconvenience when simulating closed flows. Nevertheless, after the flow achieves steady

[‡]Not in 1D problems.

state, those invariants stabilize and oscillate around established values, and do not suffer from random walks typical for non-conservative spatial weights. Thus, the approach may be called quasi-conservative.

Repeated collisions. The distortion caused by the limited number of simulators is interrelated [17] with the probability of repeated collisions (i.e., two simulators collide twice without colliding other simulators in between), thus, the fraction of repeated collisions may serve as measure of statistical dependence between simulators, which spoils the assumption of molecular chaos. In [10], an estimation of this probability p_{rpt} is proposed, that yields $\sim h/(\lambda\overline{N})$ discretization index in the simplest case:

$$p_{rpt} \sim \overline{v_{ij} t_p} \sim \frac{F\overline{\sigma_T c_r}}{V_C} \cdot t_p, \tag{1.4a}$$

$$t_p \sim \frac{h}{\overline{c_r}}, \tag{1.4b}$$

$$p_{rpt} \sim \frac{F\overline{\sigma_T c_r}}{V_C} \cdot \frac{h}{\overline{c_r}} \sim \frac{F\overline{\sigma_T} h}{V_C}, \tag{1.4c}$$

$$\frac{F\overline{\sigma_T} h}{V_C} = \frac{n\overline{\sigma_T} h}{nV_C/F} = \frac{\sqrt{2} n\overline{\sigma_T} h}{\sqrt{2}\cdot\overline{N}} = \frac{1}{\sqrt{2}} \cdot \frac{h}{\lambda\overline{N}}. \tag{1.4d}$$

Here t_p is an estimate of the time a pair of just collided simulators needs to separate far enough not to gather in the same cell and collide again. It is assumed $\Delta t < t_p$, i.e., simulators don't separate faster than 1-2 cells per time step. Simulators need at least one time step to separate, so, with $\Delta t > t_p$, an effective value of t_p becomes Δt. In result, p_{rpt} rises linearly with Δt [10] and the distortion caused by the limited number of simulators increases. Thus, if very small cells are used, the time step must be small enough as well. This is important for 1D problems, when $h/(\lambda\overline{N})$ is invariant on cell size.

For gas mixtures, p_{rpt} is different for collisions between different components, being higher for collisions with larger cross-section. In the case when component weights are used, p_{rpt} is different for two simulators from a pair. For component A, the weight F_B of component B should be used to estimate p_{rpt} in $A-B$ collisions, and vice-versa. Thus, component weights are useful not only to amplify a scarce component, but also to use more simulators only for components with bigger collision diameter.

The per-component time step approach introduced in this paper is a new tool useful to simulate flows where each component has a different characteristic time. For example, consider a binary gas mixture of a light carrier component A and a small amount of large polyatomic component B (a typical case in supersonic deposition experiments [18], when deposited precursor molecules need to be accelerated to high velocity). The $A-B$ collision cross-section is usually much larger than $A-A$. As a result, B has a much greater collision rate than A, sometimes forcing to decrease a single global time step (especially if B consists mostly of light atoms). Additionally, as was shown above, a large $A-B$ collision cross-section forces to use more simulators for A, otherwise B will suffer from frequent repeated collisions with A. This is true even if the concentration of admixture B

is small enough not to disturb the flow of carrier gas A, despite the fact that simulating the carrier A alone may be done with a smaller number of simulators.

Fortunately, the new approach allows to decrease only the time step for component B. Besides, less simulators of component A are required when component B is slowed down. This new approach works only for stationary flows.

2 Per-component time step

Let us start by sketching the Boltzmann equations for binary mixture of components A and B:

$$\begin{cases} \dfrac{1}{T_A}\cdot\dfrac{\partial f_A}{\partial t}+v_i\dfrac{\partial f_A}{\partial x_i}=F_A\cdot I_{AA}[f_A,f_A]+F_B\cdot I_{AB}[f_A,f_B], \\ \dfrac{1}{T_B}\cdot\dfrac{\partial f_B}{\partial t}+v_i\dfrac{\partial f_B}{\partial x_i}=F_B\cdot I_{BB}[f_B,f_B]+F_A\cdot I_{BA}[f_B,f_A]. \end{cases}$$

Here f_A and f_B are distribution functions of simulators for components A and B, dependent on velocity vector v_i and coordinates x_i. Functionals I_{AA}, I_{AB}, I_{BA}, I_{BB} are standard collision integrals. F_A and F_B are component weights, i.e., number of real molecules per simulator. T_A and T_B are time scaling factors, which should both be equal to unity for the standard Boltzmann equation. However, when a steady state is achieved, temporal derivations become zero, and equations are satisfied with arbitrary values of time scaling factors. Equations may be written in different form:

$$\begin{cases} \dfrac{\partial f_A}{\partial t}+(T_Av_i)\dfrac{\partial f_A}{\partial x_i}=T_A^2\cdot W_A\cdot I_{AA}[f_A,f_A]+T_AT_B\cdot W_B\cdot I_{AB}[f_A,f_B], \\ \dfrac{\partial f_B}{\partial t}+(T_Bv_i)\dfrac{\partial f_B}{\partial x_i}=T_B^2\cdot W_B\cdot I_{BB}[f_B,f_B]+T_AT_B\cdot W_A\cdot I_{BA}[f_B,f_A], \end{cases}$$
$$W_A=\frac{F_A}{T_A},\qquad W_B=\frac{F_B}{T_B}.$$

This form gives a hint about modifying the simulation scheme. First, the transposition phase should scale the global time step with the given time step scaling factor $_i$, just like in Kannenberg's approach. Second, collisions between simulators of the same component may be treated the same way as in Kannenberg's approach (1.3). Third, a more generalized version of (1.2) for inter-component collisions should be used:

$$v_{ij}=T_AT_B\frac{\max\{W_A,W_B\}\sigma_Tc_r}{V_C}.$$

Again, if two components have different combined weights (i.e., $W_A\neq W_B$), the one with smaller combined weight always receives post-collision parameters and the other does so with probability $\min\{W_A,W_B\}/\max\{W_A,W_B\}$. If combined weights are equal, both

simulators always change their parameters in a collision; hence, the collision scheme is symmetrical and quasi-conservative in this case.

As in Kannenberg's scheme, time step scaling factors may change from cell to cell– moreover, now time step scaling factors of various components may change independently, adapting to local characteristic times.

When spatial weights are used as well, so that either F and/or W includes explicit dependence on coordinates, the simulator duplication/decimation should be applied when the combined weight W at the end of displacement trajectory is different to that at the beginning. Note, the ratio of old and new W, not the ratio of F, should be used in duplication/decimation procedure.

When collecting samples inside cells by snapshots (summing parameters of simulators inside), the component weight F should be used to scale the contribution of a simulator. When collecting samples on simulators hitting or crossing some surface or boundary, as well as determining the number of simulators to inject from boundaries, the combined weight W should be used instead.

Now let us examine the repeated collision probability and extend (1.4) to the case when different time steps for components A and B are used. Again, let A be the light carrier gas with the mass m_A and B be the heavy admixture with the mass $m_B = \mathcal{M} \cdot m_A$, with $\mathcal{M} \gg 1$ being the mass ratio. The probability of repeated collision for component B is:

$$p_{rptB} \sim \frac{F_A \sigma_{AB} h}{V_C} \cdot \left\langle \frac{T_B \cdot \|\overrightarrow{v_A} - \overrightarrow{v_B}\|}{\|\overrightarrow{v_A} T_A - \overrightarrow{v_B} T_B\|_D} \right\rangle. \tag{2.1}$$

For component A, just swap indexes A and B. The index D means that only those vector components that lie in the computational domain subspace should be taken into account (i.e., only one in 1D case, 2 in 2D case, and all 3 in 3D case). The worst case is when $\|\overrightarrow{v_A} T_A - \overrightarrow{v_B} T_B\|_D \to 0$, though it is unlikely and may be avoided by choosing slightly different time step scaling factors when flow predisposition to adverse component velocity ratio is expected.

Let us examine the simplest case, when mean velocities may be assumed to be zero, and only thermal velocities contribute. Thermal velocities in equilibrium are in proportion to the reciprocal square root of molecular mass. Eq. (2.1) and its version for A then becomes:

$$p_{rptB} \sim \frac{F_A \sigma_{AB} h}{V_C} \cdot \sqrt{\frac{1+\frac{1}{\mathcal{M}}}{\frac{1}{\mathcal{M}} + \left(\frac{T_A}{T_B}\right)^2}} = \frac{T_B W_A \sigma_{AB} h}{V_C} \sqrt{\frac{1+\frac{1}{\mathcal{M}}}{1+\frac{1}{\mathcal{M}} \cdot \left(\frac{T_B}{T_A}\right)^2}}, \tag{2.2a}$$

$$p_{rptA} \sim \frac{F_B \sigma_{AB} h}{V_C} \cdot \sqrt{\frac{1+\frac{1}{\mathcal{M}}}{1+\frac{1}{\mathcal{M}} \cdot \left(\frac{T_B}{T_A}\right)^2}} = \frac{T_A W_B \sigma_{AB} h}{V_C} \sqrt{\frac{1+\frac{1}{\mathcal{M}}}{\frac{1}{\mathcal{M}} + \left(\frac{T_A}{T_B}\right)^2}}. \tag{2.2b}$$

As seen from (2.2a), slowing down heavy component B with respect to light A, favors the decrease of repeated collisions for B. Contrary, accelerating B causes more repeated collisions, up to $\sqrt{\mathcal{M}+1}$ times. Slowing down A with respect to B, but keeping the same W_A

(i.e., balancing the slow-down by proportionally increasing the number of simulators) is safe and does not cause more repeated collisions.

Now the light component (2.2b): both slowing down and accelerating A is safe. Slowing down B is safe as well. Accelerating component B while keeping the same W_B (i.e., proportionally decreasing its number of simulators) causes more repeated collisions for A, up to $\sqrt{\mathcal{M}+1}$ times.

Thus, after combining both analyses, slowing down the heavy component is safe with respect to $A-B$ collisions, while slowing down the light component is safe only when balanced by the proportional increase in its number of simulators. Accelerating the light component is safe and allows decreasing its number of simulators proportionally. Accelerating the heavy component is unsafe and not recommended.

The effect of time scaling factors and combined weights on $A-A$ and $B-B$ collisions should not be overlooked as well and must be checked separately. Also, simulators should not separate by too many cells per time step. With different time steps for two components, it is now more probable in supersonic flows.

Though (2.2a) and (2.2b) are derived for zero mean velocities and equilibrium only, I use them as universal hint in my simulations and it seems to work well. Further computational investigations of the effect of selection of time step scaling factors are encouraged.

3 A test of slowing down the light component

A good model problem for the test is the classic 1D heat transfer problem: a gas is contained between two parallel plates of different temperature, the molecules experience full accommodation of momentum and energy on both plates, the heat flux between the plates is measured. It is well-known that even a small admixture of a light gas to a heavy one may noticeably increase the heat conductivity of a mixture because of the faster thermal speed of the light component. For the test, let's take a model mixture of 10% He +90% Xe. The heat conductivity of such a mixture is $\approx$1.5 times higher than that of pure xenon. Helium's thermal speed is ≈ 6 times higher, and the collision rate is ≈ 2 times higher, in comparison with xenon.

The test will consist of simulating the heat transfer problem with three different time step factors T_H for helium: 1 (standard DSMC), 1/1.7 and 1/3. Slowing down helium is balanced by the proportional increase in the number of simulators for it (keeping combined weight constant), thereby, quasi-conservative mode is provided. The wall heat flux q is determined by sampling all the simulators colliding with walls, and dependence of heat flux deviation on the global time step is to be studied. The Variable Soft Spheres (VSS) collision model is used with Bird's parameters [1] for all three types of collisions. The temperatures of the walls are set 137K and 536K — fourfold difference (the former one is lower than the freezing point 161K of real xenon, but it does not matter for this numeric test). The distance between walls and the gas density correspond to the chosen value of the similarity parameter: $Kn_0 = 1/(\sqrt{2}n_0\sigma_{(H-H)}L) = 0.1$, here n_0 is the total

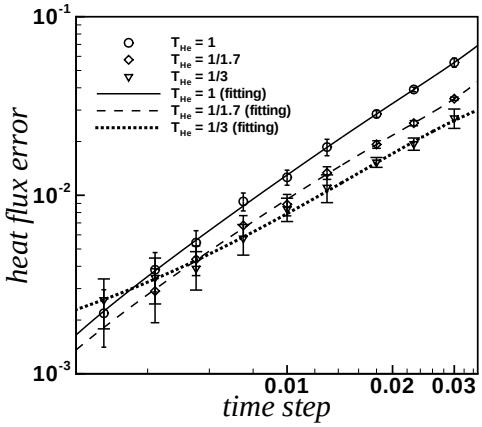

Figure 1: Dependence of heat flux error on global time step, with different time step scaling of light component (helium). Actual points and fitted curves.

number density of the mixture, $\sigma_{(H-H)}$ is the helium-helium collision cross-section, both determined at isothermic initial condition (273K), L is the distance between walls. The distance is divided by 500 uniform cells. The numbers of simulators are: 5000 for $T_H=1$, 5350 for $T_H=1/1.7$, and 6000 for $T_H=1/3$.

Results of three series of simulations are shown in Fig. 1. The unit of time equals: $L/(753m/s)$. The "reference" value of heat flux q_{ref} was determined using time step of 0.001, the deviation is calculated as: $|q/q_{ref}-1|$. Actual points acquired by simulations are shown together with fitted curves. One can see that slowing down helium 1.7 times allows increasing the global time step by 25%, keeping the deviation under 1%, at the cost of 7% more total simulators, while keeping the same global time step decreases the heat flux deviation by 25%. Slowing down helium 3 times allows increasing the global time step by 50%, at the cost of 20% more simulators, or decreases deviation by 35% keeping the same global time step.

This test confirms that slowing down the light admixture component may improve the precision of simulation. It keeps true down to minor time steps, where the deviation cannot be resolved correctly.

4 A test of slowing down the heavy component

For this test, a good model problem is a supersonic flow of a mixture around an obstacle, with shock wave and compressed layer formed in front of an obstacle, and the heavy component decelerating in the compressed layer (because of disparate masses, relaxation between light and heavy molecules needs many collisions). Such a problem needs at least a 2D simulation domain. However, 1D problems are simpler, have less parameters and allow to collect better statistics. The simplified 1D problem is following. Consider a gas mixture confined between two parallel plates, which model the bounds of a compressed

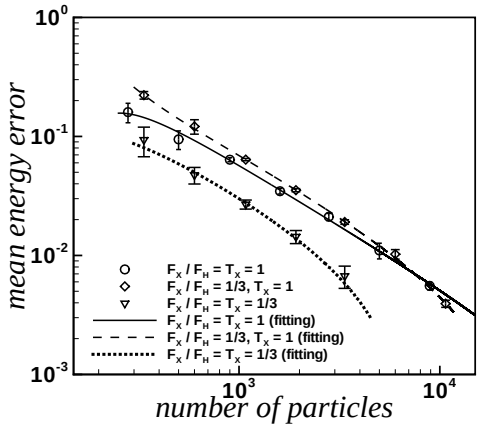

Figure 2: Dependence of mean heavy component (xenon) energy after passing "compressed layer" on the total number of simulators, for different time step scaling of heavy component. Actual points and fitted curves.

layer, with the left one being a "shock wave", and the right one a "target". The light component is diffusely reflected from both walls with full accommodation of energy and momentum. The heavy component reflects diffusely from left plane only. If a heavy molecule hits the right wall, it is considered as "deposited" and leaves the computation domain. As soon as it happens, a new heavy molecule is reemitted from the left boundary with high velocity, being considered as just "having entered" the compressed layer from a supersonic jet. Thus, the number of molecules in the simulation domain is constant. The mean energy E of heavy molecules reaching the right plate is studied.

Both plates are kept at 273K. The mixture is 90% He + 10% Xe. Again, the VSS model with parameters [1] is used. The similarity parameter: $Kn_0 = 1/(\sqrt{2}n_0\sigma_{H-H}L) = 0.04$. Xenon molecules are injected with zero temperature and a velocity of $1684 m/s$. The distance between plates is divided by 500 uniform cells. The global time step equals $0.001 \cdot l/(753 m/s)$. The varied parameter is the total number of simulators, by means of changing the combined weight. Three series of simulations are made: xenon time step scaling factor $T_X = 1$ and ratio of component weights $F_X/F_H = 1$ (standard DSMC), $F_X/F_H = T_X = 1/3$ (xenon is slowed down, its number of simulators is increased proportionally) and $F_X/F_H = 1/3$ with $T_X = 1$ (number of xenon simulators is increased, but time step is the same, non-conservative mode). In the latter two cases, 20% more total simulators are used. The "reference" energy is computed with standard DSMC using 300,000 simulators. Then, the deviation is computed as follows: $\|E/E_{ref} - 1\|$.

Results are plotted in Fig. 2. One can see that when different time steps are used, the mean energy error decreases to less than half of that of standard DSMC. Or, the same error may be achieved halving the number of simulators. Using just different component weights, without time step scaling, does not give such an improvement of precision. This is predictable and testifies that improvement is caused by using different time steps, not by changing the portion of xenon simulators.

The test confirms that slowing down a heavy admixture component may improve the precision of simulation as well.

5 A qualitative test in 2D

One more test of slowing down the heavy component, but full 2D simulations are used this time. Again, let us choose the problem of the deceleration of a heavy admixture in the compressed layer formed by the carrier gas in front of the flat plate [19]. However, this time let's just do the qualitative comparison and do not analyze the behavior of some error value. For this to be possible, let's advisedly use bare number of simulators.

The problem setting for the test is as follows. Consider the supersonic plane-parallel flow of a gas mixture, consisting of 95% He +5% Xe, with temperature of 29.25K and speed of $V_\infty = 1592 m/s$. This corresponds to the stagnation temperature of 660K and the Mach number of 8.05. The flat plate of the width L is placed perpendicularly to the flow. The plate temperature is 273K, both components diffusely scatter from both sides of the plate, with full accommodation. The characteristic Knudsen number: $Kn_\infty = 1/(\sqrt{2} n_\infty \sigma_{H-H} L) = 1$. Here n_∞ is the total number density in undisturbed flow, σ_{H-H} is the helium-helium collision cross-section at 273K (collision diameter is 2.3$\mathring{A}$).

The energy spectrum of heavy molecules hitting the front side of the plate is observed. The typical energy spectrum under these conditions consists of three contributions: the high-energy part of xenon molecules came from undisturbed flow and decelerated by multiple collisions with helium in the compressed layer, the low-energy part of xenon molecules collided with the plate before and then with helium and the middle-energy part of xenon molecules came from collisions between low-energy and high-energy xenon.

The cell size is $h = 0.025 \cdot L$. The number of simulators is defined by: $\sqrt{2} F_H \sigma_{H-H} h = 0.5$. Four simulations are made: standard DSMC ($F_X/F_H = T_X = 1$), DSMC with component weights ($F_X/F_H = 0.15$), new approach in quasi-conservative mode ($F_X/F_H = T_X = 0.15$), and the reference simulation–standard DSMC with $25x$ number of simulators.

Fig. 3 presents the high-energy part of energy spectra for these cases. The unit of energy is $m_X V_\infty^2/2$, with m_X being mass of xenon (131a.u.), the integral flux density is normalized to the flux density $n_X V_\infty$ in undisturbed flow, with n_X being number density of xenon. One can see, standard DSMC shows the most deviation from the reference spectrum, the new approach shows the least deviation, the DSMC with component weights is better than standard DSMC, but worse than the new approach. In the latter case, using the component weights for xenon improves the simulation of xenon-xenon collisions, but xenon-helium collisions are of the same quality as in standard DSMC. In contrast, the new approach improves the simulation of xenon-helium collisions as well as of xenon-xenon, though it needs more time steps to collect good averages.

Fig. 4 shows the temperature of xenon. This temperature reaches high values (over 3500K) and is non-physical because of high non-equilibrium in the rarefied compressed

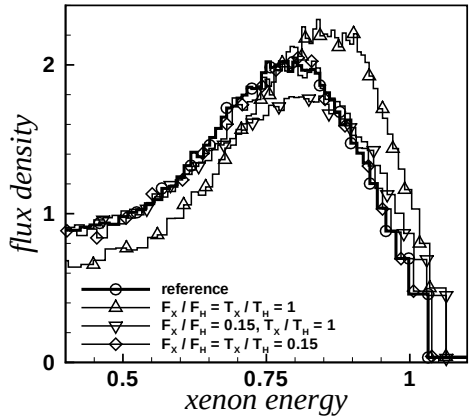

Figure 3: High-energy part of energy spectrum of xenon simulators hitting the target, for simulations with different settings.

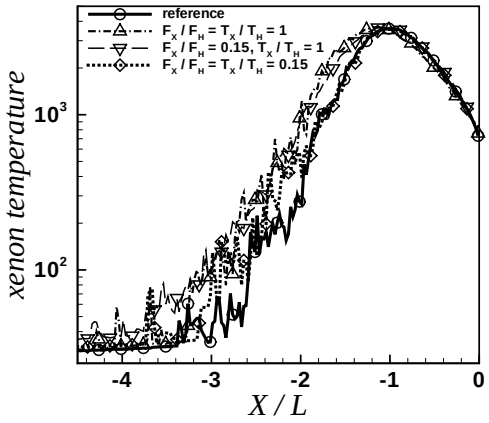

Figure 4: Translational temperature profile of heavy component at the plane of symmetry, for simulations with different settings.

layer, though it still characterizes the thermal energy of xenon, as some high-energy xenon-xenon collisions do happen. Again, the new approach gives the values closest to reference simulation. At $X/L<-3$, the non-conservative approach of component weights shows its usual artifact of overestimating the temperature of the amplified heavy component.

The test confirms that the new approach can improve complex 2D simulations of disparate mass gas mixture flows as well.

6 Simulating diffusion of silver nanoclusters in argon flow

After testing the new approach on simple problems, it is time to demonstrate its use under conditions of a real application. Considered as good problem for the new approach

would be the silver nanocluster diffusion in transonic flow of argon carrier gas. This problem refers to numeric analysis of bactericide silver-fluoropolymer coatings deposition experiments [20] performed in the Kutateladze Institute of Thermophysics SB RAS (Novosibirsk, Russia). Simulations are performed under conditions of one of routine experiments, where the source of fluoropolymer precursor is inactive, and only a flow from the silver vapor source contributes to deposition. As is known from experiments, in this case the coating is formed generally from silver nanoclusters formed inside the silver vapor source. Two fractions of silver particles are involved: small nanoclusters of few nanometers in diameter and nanoparticles of tens of nm.

Profiles of nanocluster flow in front of the surface for some fractions of nanoclusters are obtained from simulations. The experimental team has kindly agreed to set up an additional experiment of silver deposition onto a fixed long narrow stainless steel plate, so the profile of the coating can be examined as well and compared with simulation results.

An axisymmetric problem setting is used in the simulation. Standard radial spatial weighting is used to level the number of simulators at different radii. Kannenberg's approach is used to reduce computational demand in low-density areas, i.e., few regions of different cell size and time step are used. In the stagnation chamber, the cell is $30\mu m$ and the time step is $40ns$. Outside the source, the cell size and time step are 3.5 times larger. The number of simulators is chosen so that $h/(\lambda\overline{N})=0.04$ near the silver surface, $\sim$1,700,000 of argon simulators are present simultaneously in the simulation domain.

Nanocluster fractions of 16, 64, 256 and 1024 silver atoms are chosen for simulation. The concentration of nanoclusters is considered low enough not to disturb the argon and not to collide with each other, i.e., component weights are used, the argon simulator velocity never changes in argon-nanocluster collisions, thus, nanoclusters act like test particles. With the new approach used, nanoclusters are slowed down up to 25 times. The hard sphere collision model is used for all Ar–nanocluster pairs, the Borgnakke-Larsen model is used for internal degrees of freedom, with all collisions being non-elastic. The summary of molecular model parameters is shown in Table 1.

Table 1: Model parameters for different components.

Component	VSS model parameters for collisions with argon, $T_{ref}=950^\circ C$			Mass, a. u.	Internal degrees of freedom	Time step scaling factor
	D_{ref}, Å	ω	α			
Ar	3.28	0.65	1.28	40	0	1
Ag_{16}	5.66	0.5	1	1728	87	0.33
Ag_{64}	8.02	0.5	1	6912	375	0.15
Ag_{256}	11.77	0.5	1	27648	1527	0.1
Ag_{1024}	17.72	0.5	1	110592	6135	0.04

Fig. 5 shows the geometry of the problem setting, together with temperature field and streamlines of carrier gas (argon). The cylindrical stagnation chamber is on the left.

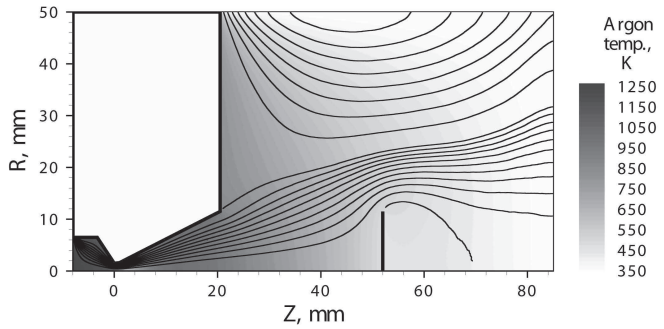

Figure 5: Streamlines and temperature field of carrier argon flow.

Its left end is the surface of a melt silver surface at 1263K. The heated carrier gas with the temperature 1213K is injected via a $1mm$ wide circular slit (6 evenly spaced holes in experiment) just above the silver surface. At $Z=-7mm$, the crucible mug part is connected with the nozzle part. From $Z=-7mm$ and up to $Z=0$ is the subsonic part of the nozzle, having the temperature of 1163 K. The small capillary at $Z=0-1mm$ is 1073K. From $Z=1mm$ and up to $Z=20.5mm$ is the divergent part of the nozzle, having a temperature of 1010K. The diameter of the stagnation chamber is 13 mm, the diameter of the nozzle critical section is $3mm$, and the diameter of the nozzle exit is $23mm$. The wall at $Z=20.5mm$ is the last heat shield, its temperature is set to 846K. Instead of the narrow plate target (about $1cm$ in width), the disk of $23mm$ in diameter is used in simulation, placed at $Z=52mm$ and having temperature of 720K. $Z=85mm$ is the right end of the computational domain, the diameter of the computational domain is $100mm$.

The pressure in the stagnation chamber is 2.1 torr, and the background pressure outside of the source is 0.14 torr. The background pressure was maintained in simulation by setting stream boundary conditions at the right and upper bounds, with given pressure, zero velocity, and temperature of 320K. One may see a noticeable distortion of argon streamlines and temperature by these boundary conditions, yet, it does not ruin the purpose of simulation. The flow of argon is injected into the settling chamber, passes and leaves the supersonic nozzle, carries the background gas along, turns around the target, and leaves the computation domain. Streamlines are drawn such that the argon flux between them is approximately the same (10%). At the plane of the target disk, the radius of the jet is about $23-25mm$. A vortex is formed behind the target.

In the divergent part of the nozzle, the flow decelerates soon after reaching supersonic speed. No pronounced shock waves are formed, because of high rarefaction. Argon mean free path is $\approx 0.13mm$ in the settling chamber, $\approx 0.2mm$ in the critical section and $\approx 0.6mm$ at the target.

Now, the nanoclusters. In this simulation, nanoclusters are supposed to form heterogeneously on the surface of convergent part of the nozzle, which have substantially lower temperature than the crucible with melt silver. They are "evaporated" from the surface, according to a Maxwellian velocity distribution (like from inlet flow of zero velocity).

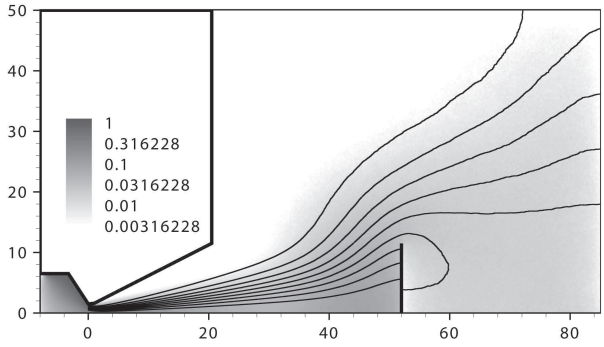

Figure 6: Density field and streamlines of Ag_{64} nanoclusters born in the settling chamber.

While argon reflects diffusively from walls and target, nanoclusters are considered adsorbing on them, as well as on open bounds of computational domain. Rarefied argon flow is perceived much denser by larger nanoclusters. For example, the collision rate of Ag_{1024} is 20 times greater in comparison with argon, and the mean free path of Ag_{1024} in the stagnation chamber is less than $100nm$ ($\approx$1000 times less than of argon). On the other hand, nearly 2000 collisions with argon are needed to lose 50% of momentum. The diffusion coefficient of Ag_{1024} is about 50 times less in comparison to self-diffusion of argon (and about 35 times less than the diffusion coefficient for silver vapor).

Fig. 6 shows the structure of the Ag_{64} flow from the stagnation chamber. Streamlines are placed so that the flux between them is the same at $Z \approx 0$. Inside the chamber, streamlines are not shown, because the mean velocity of nanoclusters is too small in comparison with statistical noise. This is the typical structure of nanocluster flow from the settling chamber. First, nanoclusters, emitted by the subsonic part of the nozzle, diffuse into the argon boundary layer and are slowly carried towards the nozzle throat. Most of these nanoclusters will be adsorbed back onto the emitting surface or somewhere else in the settling chamber. Remaining nanoclusters are accelerated up to very high speed (in comparison with their thermal velocity). After moving to slow subsonic flow past the nozzle, fast nanoclusters behave like macroscopic particles; they advance through the argon, gradually loosing speed with each collision. When they slow down to thermal velocity, the transition to diffusion mode happens ($Z \approx 35mm$ for Ag_{64}). Finally, nanoclusters suffer regular diffusion through argon like normal admixture molecules again. Some of them reach the front side of the target; some diffuse behind it and reach its back side.

For Ag_{16}, the transition to diffusive mode happens at the nozzle exit, for Ag_{256}, transition happens just in front of the target, and Ag_{1024} (Fig. 7) hits the front side of the target before the transition happens. Only few simulators of Ag_{1024} reached the back side of the target.

Because of its high mass, Ag_{1024} does not decelerate down to thermal velocity $(12m/s)$ in front of the target, but only down to $105m/s$. Together with high internal heat capacity, this causes an elevated internal temperature of nanoclusters when they hit the target. That might be important during the bactericide metal-polymer film deposition process,

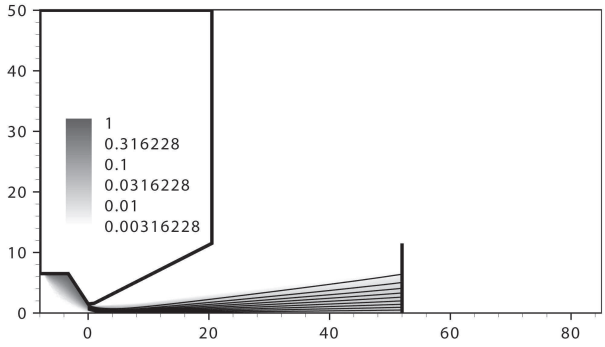

Figure 7: Density field and streamlines of Ag_{1024} nanoclusters born in the settling chamber.

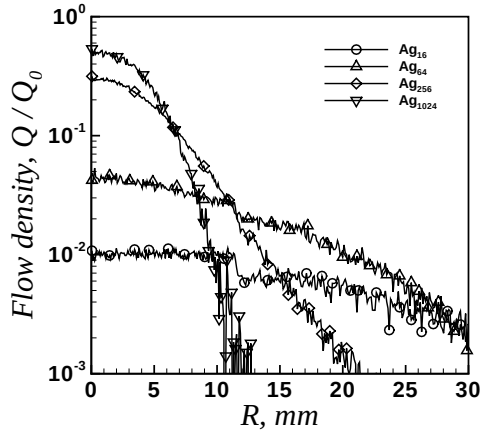

Figure 8: Flux density profiles for different nanoclusters at the plane of the target, referred to corresponding surface densities of emission.

because hot silver nanoclusters may chemically react with fluoropolymer on the target surface and thus affect bactericidal properties of the coating. However, one should also take into account a very high surface energy of nanoclusters as well, especially of smaller ones; it may be released locally if a nanocluster merges with another one on the target surface.

Fig. 8 shows flux density profiles of different nanoclusters in front of the target. As one can see, the heavier the nanoclusters, the higher is the flux at $R \approx 0$, but the narrower is the beam. Profiles for Ag_{16} and Ag_{64} are about as wide as the carrying jet of argon. However, beams of Ag_{256} and, especially, Ag_{1024} have rather sharp boundaries. While the lighter two sorts of nanoclusters would deposit anywhere on the target front, the heavier two would deposit only onto the central spot.

Fig. 9 presents a photo of the target front side after the deposition experiment. The diameter of the white spot is in good agreement with the Ag_{1024} profile from Fig. 8. This supports the adequacy of the new method in modeling the diffusion of nanoclusters. The back side of the target stayed visually clear and unaffected (and was not photographed).

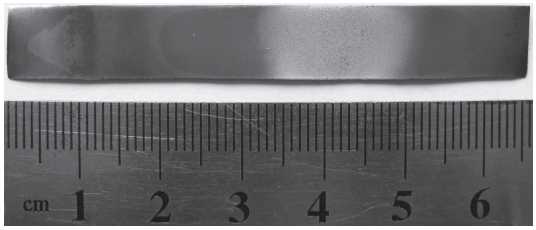

Figure 9: Photo of the target after deposition experiment.

This confirms that the majority of deposited silver comes from nanoclusters heavier than 256 atoms (otherwise, they would leave visible traces on the target back).

Note, only 1.7 million of argon simulators were used for all types of admixture nanoclusters, easy to fit in a memory of an average workstation computer. To get the same precision without using the new approach of slowing down nanoclusters, one would need over 40 million argon simulators to handle Ag_{1024}. This would significantly increase the required computational resources.

Unfortunately, simulating the diffusion of larger nanoparticles (tens of nanometers) with DSMC would be impractically expensive because of the enormous collision frequency. Nevertheless, an extrapolation of obtained results tells that nanoparticles would still form a narrow spot in the center of the target front, and not reach the back of the target. Thus, the white spot in the center of the target testifies that nanoclusters are born in the stagnation chamber. In contrary, similar simulations made for nanoclusters born on the surface of divergent part of the nozzle shows they would reach both front and back sides of the target, and heavier ones would form a ring shape.

7 Conclusions

A new approach of using a different time step in DSMC for each component was proposed, with description of algorithm changes, some recommendations on choosing appropriate component time steps and their effect on the required number of simulators. This approach was tested on a 1D heat transfer problem for a He + Xe mixture, where helium was slowed down enough not to travel too much cells per time step when global time step is increased, and on 1D and 2D variants of the problem of accelerated heavy Xe penetration through the compressed layer of light gas in front of an obstacle, where slowing down xenon allowed decreasing the number of helium simulators without a drop in simulation precision. Finally, a complex 2D axisymmetric flow was simulated for conditions of a real deposition experiment, where the coating was formed of silver nanoclusters born on inner surfaces of the silver vapor source and carried to the target by argon. The new approach made simulation possible without using an enormous number of simulators. The obtained flux profile of Ag_{1024} in front of the target turned out to be in good agreement with experimental results.

Acknowledgments

The author is grateful to A. I. Safonov and other research team members from the Institute of Thermophysics SB RAS for cooperation and providing experimental data used in Section 6.

References

[1] G. A. Bird, Molecular Gas Dynamics and the Direct Simulation of Gas Flows, Clarendon Press, 1994
[2] J. Fan and C. Shen, Statistical simulation of low-speed unidirectional flows in transition regime, Proc. 21st Intern. Symp. On Rarefied Gas Dynamics, ed. R. Brun et al., Toulouse, France, Cepadues-Editions, 2 (1998), 445.
[3] Q. Sun, Information Preservation Methods for Modeling Micro-Scale Gas Flows, PhD dissertation, Aerospace Engineering; The University of Michigan, 2003.
[4] L. L. Baker and N. G. Hadjiconstantinou, Variance reduction for Monte Carlo solutions of the Boltzmann equation, Phys. Fluids, 17(5) (2005), 051703.
[5] T. M. M. Homolle and N. G. Hadjiconstantinou, A low-variance deviational simulation Monte Carlo for the Boltzmann equation, J. Comput. Phys., 226 (2007), 2341.
[6] J.-C. Huang, K. Xu and P. Yu, A unified gas-kinetic scheme for continuum and rarefied flows II: multi-dimensional cases, Commun. Comput. Phys., 12 (2012), 662.
[7] V. A. Titarev, Efficient deterministic modelling of three-dimensional rarefied gas flows, Commun. Comput. Phys., 12 (2012), 162.
[8] F. J. Alexander, A. L. Garcia and B. J. Alder, Cell size dependence of transport coefficients in stochastic particle algorithms, Phys. Fluids, 10(1998), 1540; Erratum, Phys. Fluids, 12(3) (2000), 731.
[9] N. G. Hadjiconstantinou, Analysis of discretization in the direct simulation Monte Carlo, Phys. Fluids, 12(10) (2000), 2634.
[10] R. V. Maltsev, On the Selection of the Number of Model Particles in DSMC Computations, in Proc. 27th Intern. Symp. on Rarefied Gas Dynamics, AIP Conf. Proc. 1333 (2010), 289.
[11] J. M. Burt and I. D. Boyd, Convergence detection in direct simulation Monte Carlo calculations for steady state flows, Commun. Comput. Phys., 10 (2011), 807.
[12] M. S. Ivanov and S. V. Rogasinsky, Analysis of numerical techniques of the direct simulation Monte Carlo method in the rarefied gas dynamics, Sov. J. Numer. Anal. Math. Model, 2(6) (1988), 453.
[13] D. J. Rader, M. A. Gallis, J. R. Torczynski and W. Wagner, Direct simulation Monte Carlo convergence behavior of the hard-sphere-gas thermal conductivity for Fourier heat flow, Phys. Fluids, 18(7) (2006), 077102.
[14] G. A. Bird, Molecular Gas Dynamics, Oxford Univ. Press, 1976.
[15] A. A. Morozov and M. Yu. Plotnikov, Analysis of efficiency of some approaches of solving problems by the DSMC method, in Rarefied Gas Dynamics, Proc. 21st Intern. Symp. (Marseille, France), eds. R. Brun, R. Campargue, R. Gatignol and J.-C. Lengrand, CEPADE-EDITION, 2 (1999), 133.
[16] K. C. Kannenberg, Computational Methods for the Direct Simulation Monte Carlo Technique with Application to Plume Impingement, Ph.D. thesis, Cornell University, Ithaca, New York, 1998.

[17] A. A. Shevyrin, Ye. A. Bondar and M. S. Ivanov, Analysis of Repeated Collisions in the DSMC Method, in Proc. 24th International Symposium on Rarefied Gas Dynamics, AIP Conf. Proc. 762 (2005), 565.
[18] F. De Angelis, T. Toccoli and A. Pallaoro, et al., SuMBE based organic thin film transistors, Synthetic Metals, 146 (2004), 291.
[19] R. V. Maltsev, Inertia effects in the compressed layer in front of a flat plate, in Proc. 27th Intern. Symp. on Rarefied Gas Dynamics, AIP Conf. Proc. 1333 (2010), 295.
[20] A. K. Rebrov, A. I. Safonov and N. I. Timoshenko, et al., Gas-jet synthesis of silver-polymer films, J. Appl. Mech. Tech. Phys., 51(4) (2010), 598.